Millimeter-Gap Magnetically Insulated Transmission Line Power Flow Experiments

Brian T. Hutsel, Brian S. Stoltzfus, William E. Fowler, Peter A. Jones, David W. Justus, Keith R. LeChien, Finis W. Long, Diego J. Lucero, Keven A. MacRunnels, Michael G. Mazarakis, John L. McKenney, James K. Moore, Thomas D. Mulville, John L. Porter, Mark E. Savage, William A. Stygar

Sandia National Laboratories

Millimeter-Gap Magnetically Insulated Transmission Line Power Flow Experiments

Brian T. Hutsel, Brian S. Stoltzfus,
William E. Fowler, Keith R. LeChien, Michael G. Mazarakis,
James K. Moore, Thomas D. Mulville, Mark E. Savage, William A. Stygar
Advanced Accelerator Physics

John L. McKenney
Advanced Radiographic Technologies

Peter A. Jones, Diego J. Lucero
Pulsed Power Engineering

David W. Justus, Keven A. MacRunnels
Z Center Section and Planning

Finis W. Long
Load and Diagnostic Engineering

John L. Porter
Laser Operations and Engineering

Sandia National Laboratories
P.O. Box 5800
Albuquerque, NM 87185

Abstract

An experiment pltafrom has been designed to study vacuum power flow in magnetically insulated transmission lines (MITLs). The platform was driven by the 400-GW Mykonos-V accelerator. The experiments conducted quantify the current loss in a millimeter-gap MITL with respect to vacuum conditions in the MITL for two different gap distances, 1.0 and 1.3 mm. The current loss for each gap was measured for three different vacuum pump down times. As a ride along experiment, multiple shots were conducted with each set of hardware to determine if there was a conditioning effect to increase current delivery on subsequent shots.

The experiment results revealed large differences in performance for the 1.0 and 1.3 mm gaps. The 1.0 mm gap resulted in current loss of 40%-60% of peak current. The 1.3 mm gap resulted in current losses of less than 5% of peak current. Classical MITL models that neglect plasma expansion predict that there should be zero current loss, after magnetic insulation is established, for both of these gaps. The experiments results indicate that the vacuum pressure or pump down time did not have a significant effect on the measured current loss at vacuum pressures between 1e-4 and 1e-5 Torr. Additionally, there was not repeatable evidence of a conditioning effect that reduced current loss for subsequent full-energy shots on a given set of hardware. It should be noted that the experiments conducted likely did not have large loss contributions due to ion emission from the anode due to the relatively small current densities (25-40 kA/cm) in the MITL that limited the anode temperature rise due to ohmic heating. The results and conclusions from these experiments may have limited applicability to MITLs of high current density (>400 kA/cm) used in the convolute and load region of the Z which experience temperature increases of >400°C and generate ion emission from anode surfaces.

4

Acknowledgments

Contents

Figures

Tables

Introduction

Magnetically insulated transmission lines (MITLs) are commonly used in the final stages of pulsed power systems to transfer power at high voltage and current to the physics-package load. Areas such as the convolute and inner-MITL of the Z-Machine require MA/cm level currents to be transmitted with vacuum gaps of 1 cm or less [1]. Future pulsed power systems, which will deliver greater power to loads, will require MITLs to transfer power at greater power densities. Understanding and minimizing current loss within the MITL will be a critical design issue for these larger pulsed power systems.

MITL power flow has been studied in detail. In order to support MITL design and understand current loss in a MITL, many individual studies involving simulation [2–4], analytic calculations [5–8], and experiment [9–14] have been published.

In this Laboratory-Directed Research and Development (LDRD) project, the power flow in a millimeter-scale MITL gap was studied. The experiments performed were directed towards studying the effect of vacuum conditions on the current loss in a MITL. It is known that surface contamination alters the emission characteristics of electrodes [15, 16]. In the Z MITL system, it has been observed that increased vacuum pump down times reduces the partial pressures of electrode-surface contaminants and can reduce current loss across the MITL anode-cathode (AK) gap [17]. The experiments described in this report investigated the MITL current loss with respect to vacuum pressure in a MITL in a controlled manner, without the variability of different machine configurations or complex dynamic experiment loads that are used on Z.

The remainder of the report is divided into three sections. Section 2 covers the experiment setup including the design and layout of the pulsed power driver and vacuum hardware. Section 3 describes the results from the MITL power flow experiments. Section 4 concludes the report and describes potential future work.

Experiment Setup

Pulsed power driver

The Mykonos LTD module served as the pulsed power driver for the vacuum transmission line power flow experiments. A photograph of the Mykonos laboratory is shown in Figure 1. The vacuum transmission line power flow tests were the first experiments to be completed on an upgraded five-cavity Mykonos LTD module (Mykonos V).

Figure 1. Photograph of the Mykonos LTD laboratory.

The Mykonos V LTD module is made up of five, three-meter diameter, LTD cavities. Each cavity contains of 36 LTD bricks, each built with a HCEI 200 kV multi-gap switch [18] and two 40 nF General Atomics 31165 capacitors. The five cavities are triggered sequentially and drive a matched impedance coaxial water transmission line. The cavities are triggered with a 6.6 ns delay between cavities to match the transit time of the power pulse in the water transmission line. The cavities and water transmission line are shown in Figure 2. The LTD cavities are designed to operate at up to ±100 kV charge voltage. At full charge voltage, Mykonos V nominally produces a 1 MA, 500 kV pulse with a rise time (10-90) of 60 ns and a pulse width (FWHM) of 160 ns into a 0.5 Ω matched load. The noted references contain additional details on the Mykonos LTD cavities [19] and the two-cavity module, Mykonos II [20–22], that preceded the Mykonos V module.
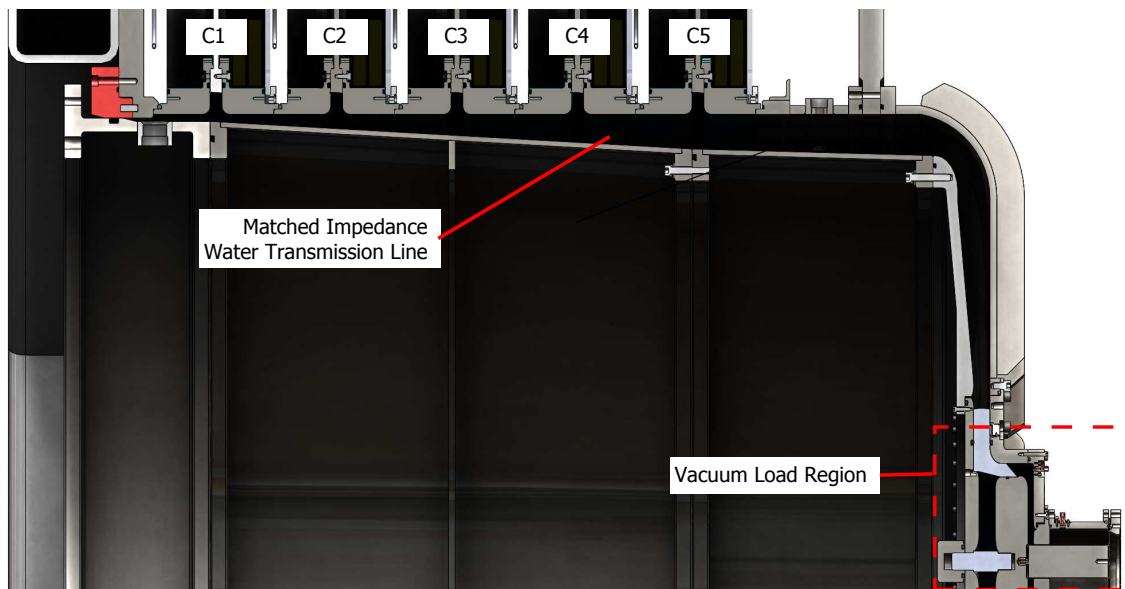
Figure 2. Cross-section view of the Mykonos V LTD module.

Load hardware design and processing

A vacuum transmission line load for Mykonos was designed and acquired for the vacuum power flow experiments. A cross-section view of the vacuum hardware is shown in Figure 3. A radial water transmission line, vacuum insulator, and radial vacuum transmission line served to direct power flow to the small diameter of the MITL being tested. The vacuum insulator serves to isolate the water-insulated transmission line from the vacuum-insulated transmission line. The vacuum insulator was also designed to direct power flow through a series water resistor. This water resistor was adjustable from approximately 0.1 Ω to 0.5 Ω and was used to dampen reflections back into the cavities from the short-circuit inductive load.

The experiment MITL consisted of a small gap, 3 cm long, coaxial vacuum transmission line. The cathode radius is fixed at 3 cm. The anode radius was either 6.2 cm or 6.26 cm in order to test AK gaps of either 1 mm or 1.3 mm. A 15 nH constant-inductance served as the load downstream of the experiment gap. The gap was designed to operate at fields of 1-3 MV/cm, well above the electron emission threshold of approximately 240 kV/cm. The cathode radius of 3 cm was chosen to minimize the inductance of the vacuum region while still ensuring magnetic insulation would be established early in the pulse, at around 200 kA.

The experiment gap anode and cathode were made of stainless steel 304L. The anode and cathode were machined with no cutting oil and electropolished per ASTM B912 standards. After machining, the hardware was cleaned with isopropanol and a TX309 Texwipe, rinsed with isopropanol and blown dry with nitrogen, vacuum baked at 800 C for four hours, then wrapped in a TX309 Texwipe and All-Foils UHV aluminum foil. The hardware was stored wrapped in the UHV foil until installed on the machine for use.
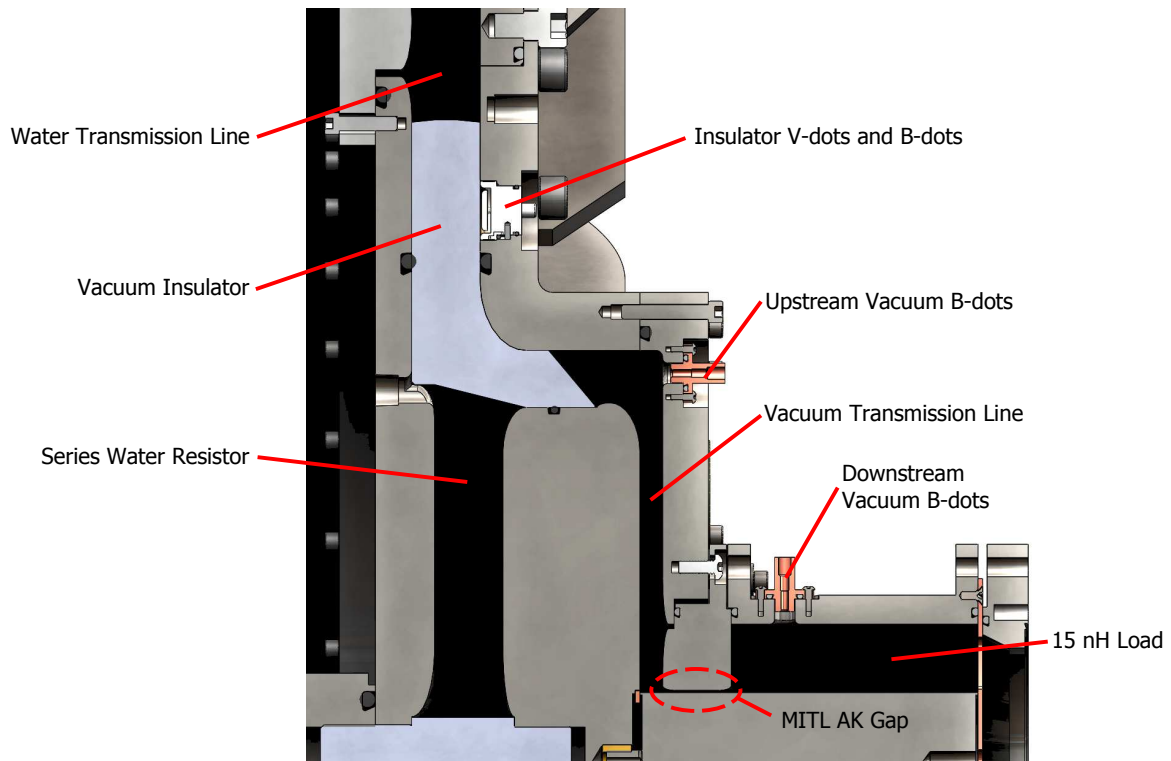
Figure 3. Cross-section view of the vacuum transmission line load hardware.

Diagnostics

The primary diagnostic included B-dot and D-dot monitors to measure current and voltage. Four B-dots and four D-dots were located at the vacuum insulator. These monitors were identical to those described in Sections III and V of [23]. In the vacuum transmission line, a total of eight B-dots were used to measure current. Four were located upstream and and four were located downstream of the experiment gap. The vacuum B-dots were designed as a 2-loop version of the inner-MITL current monitor described in Section IV of [23].

Prior to the experiments, the diagnostic monitors were calibrated in-situ. Two Pearson 3483 current monitors, accurate to $\pm 1\%$ absolute, were used in opposite polarities as calibration references for the vacuum and stack b-dot monitors. The negative polarity Pearson signal was inverted and averaged with the positive polarity Pearson signal to generate the final reference current signal. Voltage measured across a 2 kΩ resistor was used as the calibration reference for the D-dots. For calibration, the monitor signals were baseline-corrected to subtract any DC offset. The signals were then numerically integrated, and compared using an iterative routine to find the time shift and amplitude scale to minimize the point-wise rms differences between the reference waveform and the signal being calibrated. The B-dots also included a correction for the magnetic field penetration, as described in [23]. The signals gave rms point-wise deviations of a scaled signal divided by its peak of less than 1%. Ten calibration tests were averaged to generate the gauge factors. The maximum shot-to-shot variation in gauge factors was 1.7% or less. A sample calibration shot is shown in Figure 4.
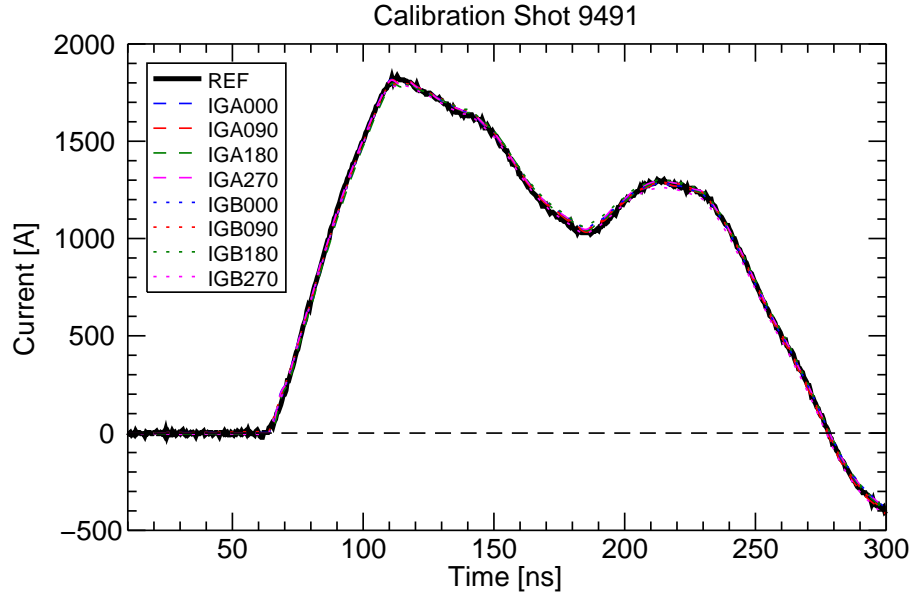
Figure 4. Baselined, integrated, flux penetration corrected, and scaled vacuum B-dot signals overlaid on the reference signal for calibration shot 9491.

13

Vacuum diagnostics included two MKS 979b full-range gauges to measure vacuum pressure upstream and downstream of the experiment gap. The reported vacuum pressure was measured by the upstream gauge. The upstream gauge was always the higher of the two vacuum measurements. This was due to a molecular pumping restriction caused by the experimental gap. The high upstream pressure was exacerbated by the vacuum seals on the insulator itself. A Stanford Research Systems RGA 100 was also available to measure the vacuum composition during pump down.

Shot procedures

The experiment gap anode and cathode were replaced for each shot series. All other vacuum hardware was reused, and refurbished if necessary. Vacuum surfaces that were coated with debris from breakdown of the experiment AK gap were refurbished with 3M Scotch-Brite surface conditioning pads. The hardware was then vacuumed and wiped with a TX309 Texwipe and ethyl alcohol. The experiment gap anode and cathode hardware that were regularly replaced were not removed from the UHV foil they were stored in after processing until they were ready to install. The AK gap was aligned to +/- 2% of nominal gap using gauge pins to verify alignment. After the anode and cathode were aligned, the remaining vacuum hardware was installed and the system was pumped down. Pump down time was varied as an experiment variable. Typically the disassembly, refurbishment, and assembly of the load hardware was completed in approximately one hour. During installation, all vacuum hardware was handled only with clean nitrile gloves.

Experiment Results

The current loss as a function of time for each experiment was determined from the B-dot diagnostics upstream and downstream of the MITL gap. Typically a small amount of loss could be measured early in the pulse. Later a sharp divergence of the upstream and downstream current measurements indicates complete closure of the MITL AK gap. At this point the downstream current slowly L/R decays as magnetic energy stored in the load inductance dissipates.

MITL AK gaps of 1.0 and 1.3 mm were tested in the experiments. These gaps exhibited very different current loss characteristics. The 1.0 mm AK gap saw early losses of approximately 60 kA, prior to when magnetic insulation would be expected. Typically this loss would hold constant for a brief time (10-30 ns) before complete closure of the AK gap occurred at 40%-60% of peak current. The time from beginning of current loss to complete closure of the AK gap ranged from 40-60 ns, corresponding to a gap closure velocity of 2e5 cm/μs. A representative shot with the 1.0 mm AK gap is shown in Figure 5. In contrast, the 1.3 mm AK gap did not close until near peak current. The early losses, prior to magnetic insulation were greatly reduced as well. A representative shot with the 1.3 mm AK gap is shown in Figure 6. These results are consistent with observations in [12], where it was noted that the gap closure time occurred in several distinct regimes depending on the MITL AK gap.

For reference, Appendix A contains a table documenting all of the shots taken for this LDRD project.

Effect of vacuum pressure

Experiments focused on characterizing the current loss dependence on the vacuum pressure in the MITL. In general, the MITL experiment gap was tested under three different vacuum conditions; a long vacuum pump down of more than 18 hours (up to 144 hours), a pump down of 2-3 hours, and a short pump down of only 10 minutes. The pressures measured by the upstream vacuum gauge were approximately 1e-5 Torr, 2e-5 Torr, and 1e-4 Torr for each these vacuum exposure times, respectively.

The results indicate that vacuum pressure did not have a significant effect on the current loss at pressures between 1e-4 and 1e-5 Torr for either the 1.0 mm or 1.3 mm gap. Figure 7 shows the results of 60 kV, 1.3 mm AK gap shots. The average loss for each vacuum pressure is shown and the error bars indicate the standard deviation of the loss. It can be seen that the average loss for shots decreased as vacuum pressure is decreased. However the differences in the mean are not statically significant and can not be attributed to the change in vacuum pressure. Additional data from 50 kV, 1.3 mm AK gap shots and 60 kV, 1.0 mm AK gap shots are shown in Figures 8 and 9. The data further supports that vacuum pressure (between 1e-4 and 1e-5 Torr) has little effect on the loss current. A single shot taken at rough vacuum pressure (86 mTorr) shown in Figure 8 demonstrates that a rough vacuum is insufficient for power flow through a MITL.
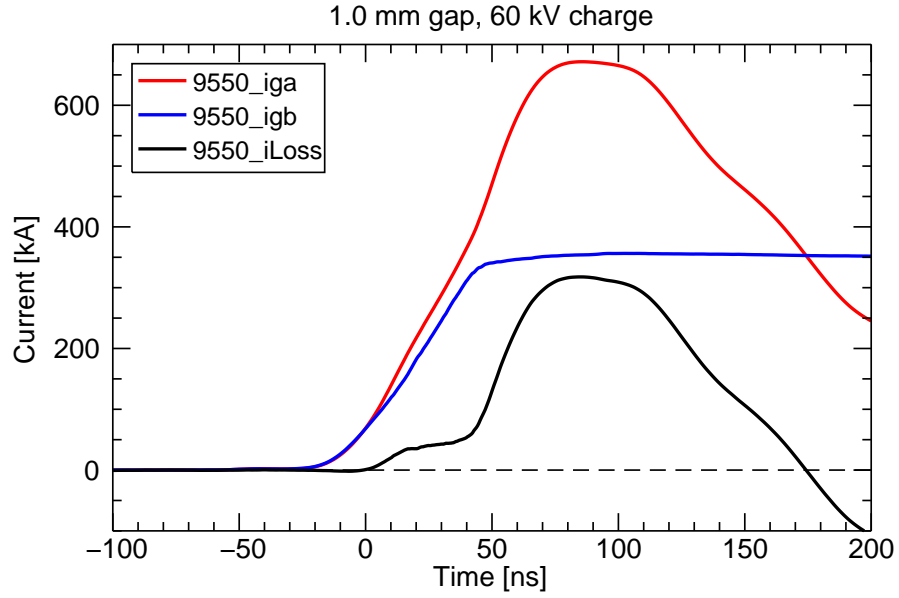
Figure 5. Typical current loss for 1.0 mm gap MITL. IGA is the current measured upstream of the experiment gap, IGB is the current measured downstream of the experiment gap and iLoss is the difference of IGA and IGB representing the loss current across the experiment gap.
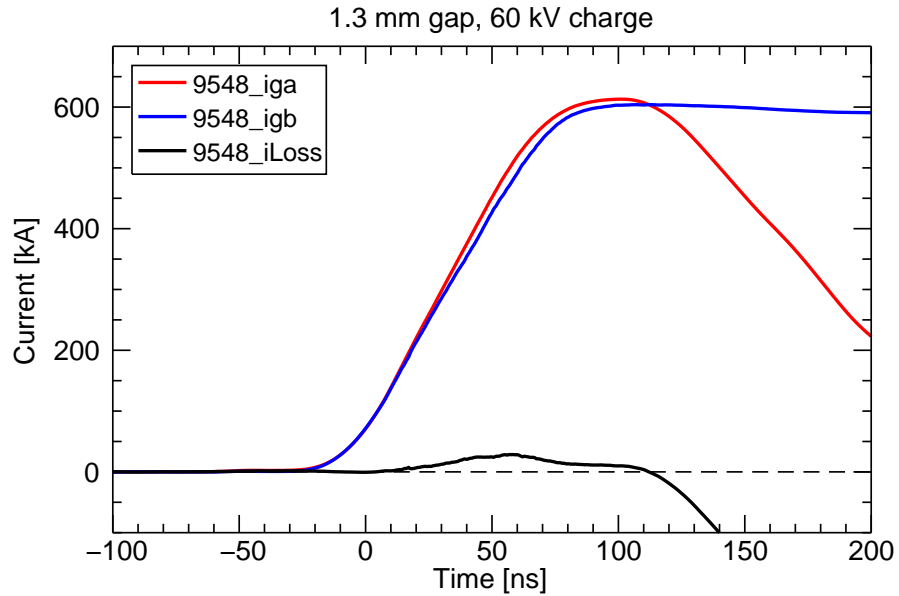
Figure 6. Typical current loss for 1.3 mm gap MITL.
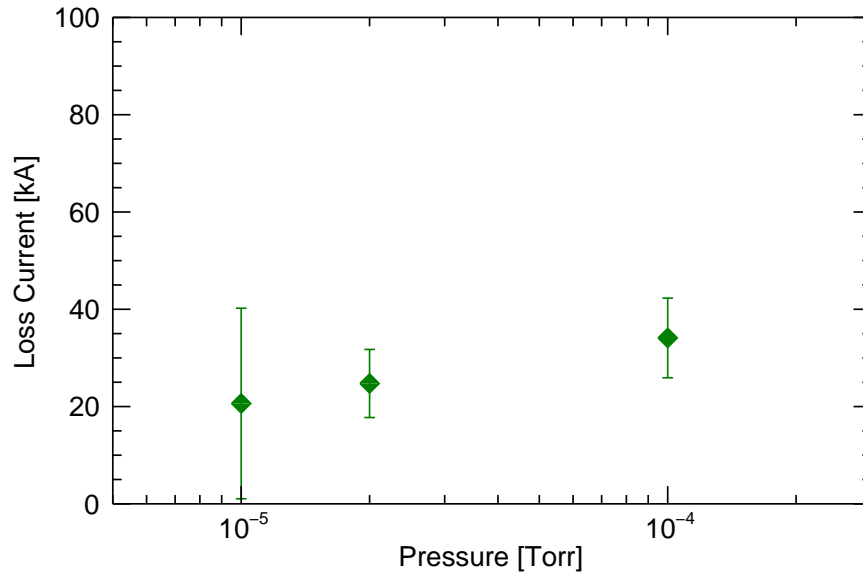
Figure 7. Current loss versus vacuum pressure for 1.3 mm gap shots taken with a charge voltage of 60 kV. Data markers represent the mean loss current and the error bars indicate the standard deviation of the data. Each marker represents at least three shots. Data shown are only from shots with new processed anode/cathode hardware.
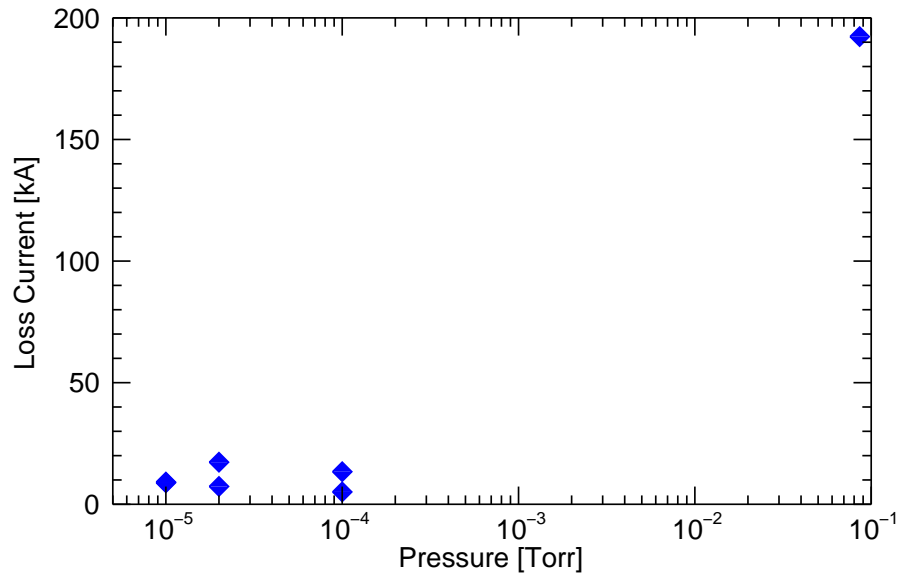
Figure 8. Current loss versus vacuum pressure for 1.3 mm gap shots taken with a charge voltage of 50 kV. Each marker represents one shot. Data shown are only from shots with new processed anode/cathode hardware.
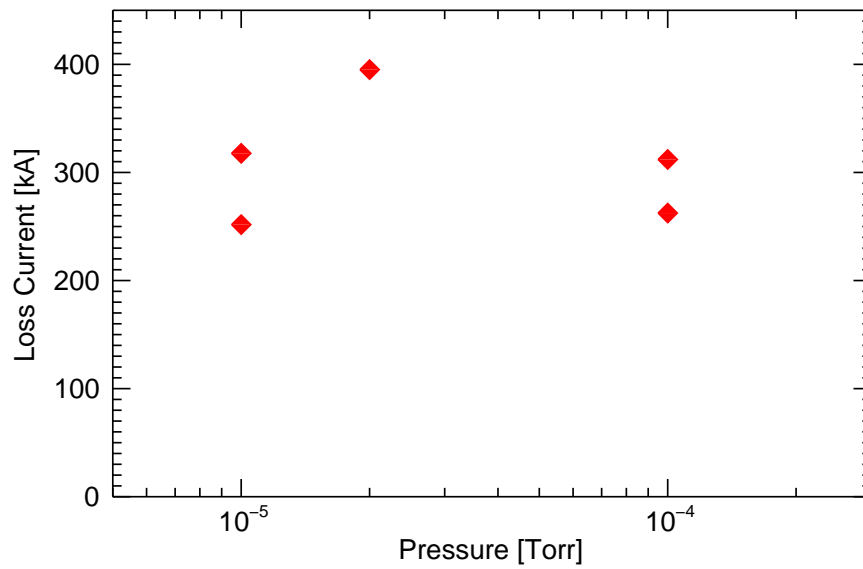
Figure 9. Current loss versus vacuum pressure for 1.0 mm gap shots taken with a charge voltage of 60 kV. Each marker represents one shot. Data shown are only from shots with new processed anode/cathode hardware.

Conditioned hardware shots

Typically, two or three shots were taken on each set of hardware. The first shot measured the current loss for new hardware. Subsequent shots on a given set of hardware were taken soon after the first shot, without breaking vacuum. These shots were conducted as a ride along experiment to determine if a conditioning effect existed which would improve power flow. A conditioning effect was noted in [12] where the authors note that the gap closure was delayed for subsequent shots, as long as the hardware remained under vacuum. It is believed that the discharges and heating from prior shots would remove electrode surface contamination, reducing the influence of electrode plasmas on the current loss.

In these experiments, there was not a repeatable indication that power flow was improved with subsequent, full-energy, shots with either the 1.0 mm or 1.3 mm gap. Figures 10 and 11 show the average and standard deviation of the current loss from the 60 kV, 1.0 and 1.3 mm gap shots. Data shown in red represents the current loss on new hardware. Data shown in blue represents the current loss on conditioned hardware. On average, the conditioned hardware resulted in a higher average loss for data sets of 2-4 shots. It is likely that the damage to the electrodes from prior shots outweighed any potential benefit of a reduction in electrode surface contamination. There is some evidence of this in two shot series, where peak current loss decreased for each subsequent shot. One example series is shown in Figure 12. It can be seen that the peak current loss decreased for each subsequent shot. However, it is also noted that the losses early in time (0-40 ns) increased for each subsequent shot. The current loss early in time, prior to magnetic insulation, could indicate that the electrode surface was degrading from damage creating a field enhancement point allowing the early time losses to turn on sooner and increase in magnitude.
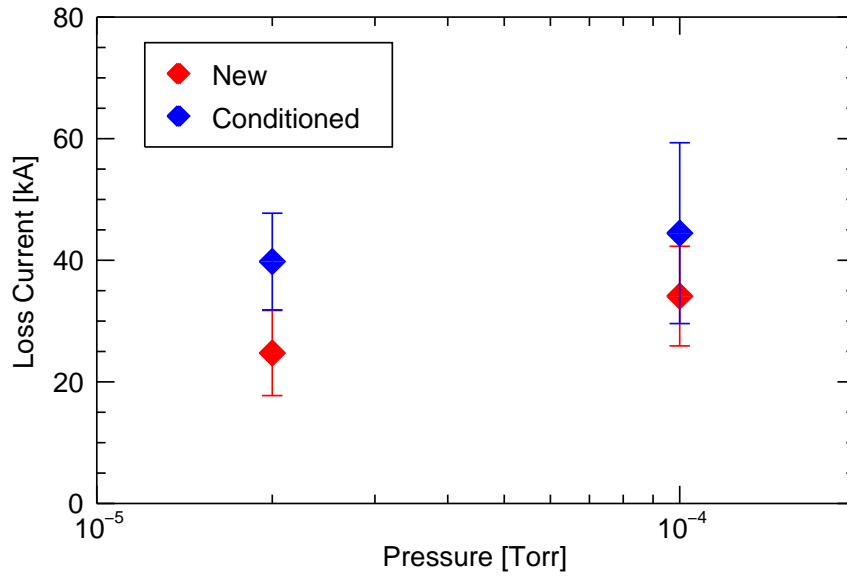
Figure 10. Comparison of current loss on new hardware and conditioned hardware for 60 kV, 1.3 mm gap. Data markers represent the mean loss current and the error bars indicate the standard deviation of the data.
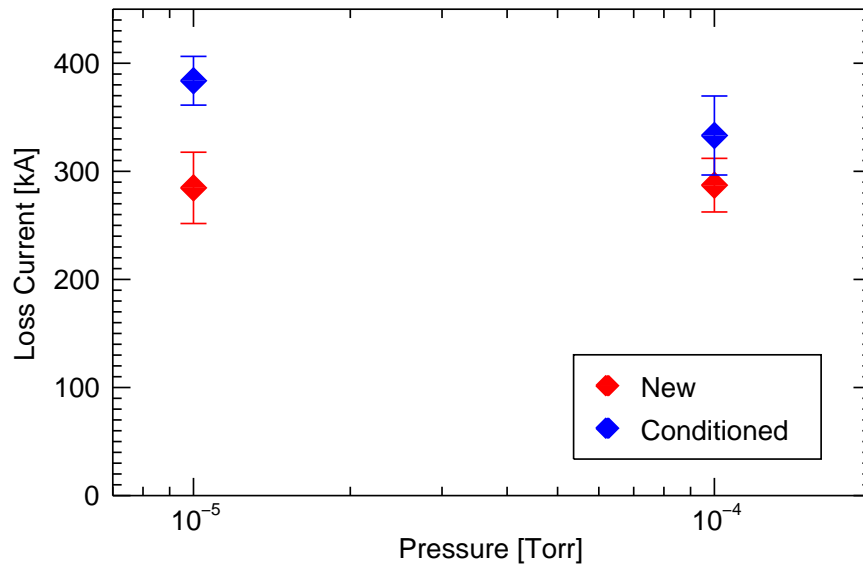
Figure 11. Comparison of current loss on new hardware and conditioned hardware for 60 kV, 1.0 mm gap. Data markers represent the mean loss current and the error bars indicate the standard deviation of the data.
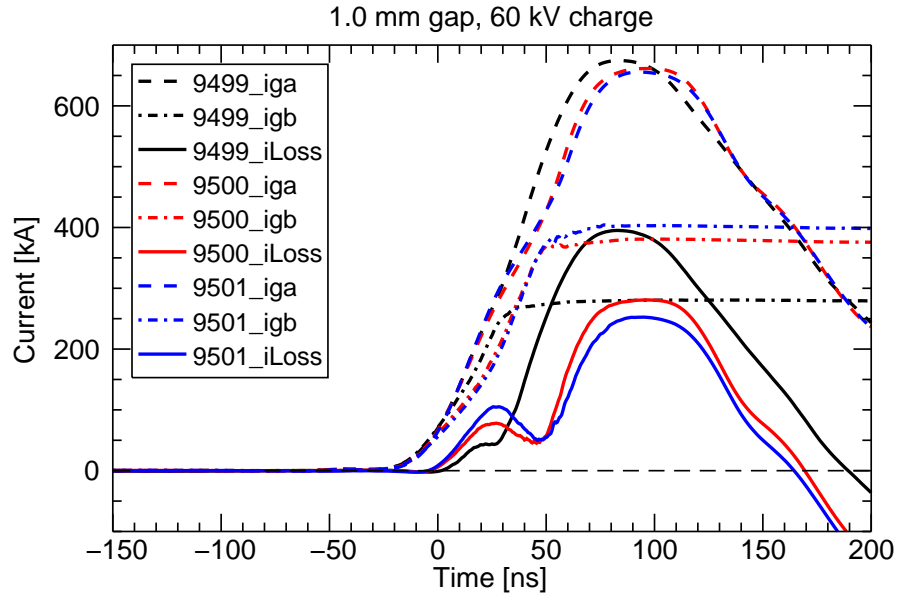
Figure 12. Current waveforms from three sequential shots taken with one set of anode/cathode hardware without breaking vacuum. The three loss current waveforms (solid lines) decrease in peak amplitude for each subsequent shot, 9499, 9500, and 9501. However losses early in time (around 25 ns) increase in time.

21

Conclusions and Future Work

Conclusion

The experiment results suggest that there is no correlation between the vacuum pressure (between 1e-4 and 1e-5 Torr) and the current loss across the millimeter-gap MITL for the conditions tested. On a given shot, a 10 minute vacuum pump down with a pressure of 1e-4 Torr could perform equally as well as a shot with a multi-day vacuum pump down with a pressure of 1e-5 Torr. This is in disagreement with the data presented for Z shots in [17] which noted that shots with longer vacuum pump down times experienced less current loss. Additionally, no evidence of electrode conditioning from full energy shots improving current delivery was observed. On average, current loss increased when subsequent shots were taken on a set of anode/cathode hardware.

The disagreement between the observations for Z shots in [17] and the results from these experiments may be a result of the limited vacuum pressures tested in these experiments or the relatively low current densities and short rise times of these experiments. The ultimate vacuum pressure achieved in these experiments was approximately 9e-6 Torr, measured upstream of the experiment gap. The low loss shots on Z were taken with vacuum pressures as low as 2e-6 Torr. Additionally, the current density in the LDRD experiments was limited to 25-40 kA/cm. The low current density in the LDRD experiments limits the temperature rise of the anode due to ohmic heating to less than $5\,^{\circ}$C, eliminating the potential for ion emission from the anode. In contrast, the inner MITL and load regions in Z have current densities in excess of 400 kA/cm and the temperature rise due to ohmic heating can be in excess of $400\,^{\circ}$C, at which point ion emission from the anode begins [16].

Future work

Additional experiments could be conducted to further the presented research. First, future experiments should be designed to reach lower ultimate vacuum pressures and also could examine the effects of additional vacuum pump down procedures, such as a dry nitrogen purge during pump down. Decreasing the pressure or implementing additional vacuum procedures would serve to reduce contaminants on the power flow surfaces and may delay plasma formation and gap closure. Second, there is interest to test alternative electrode materials. On Z, some load hardware is made from aluminum. The experiments could be repeated with aluminum anodes to determine if the current loss is significantly different with aluminum instead of stainless steel. Finally, experiments conducted with high current density, comparable to those at Z, would ensure that ion emission from the anode would contribute to the current loss. Such experiments would require a cathode diameter on the order of 0.5 cm. Additional analysis would be necessary to determine if Mykonos could drive such small diameter (high inductance) loads.

Appendix A

Table 1: The following table documents all the shots taken for the LDRD. Shot numbers in **bold** font denote shots with new anode/cathode hardware. Vac_1 refers to the pressure measurement downstream of the experiment gap. Vac_2 refers to the pressure measurement upstream of the experiment gap. Vac_2 is the vacuum pressure used when referencing a shot. I_{up} is the peak current measured by the upstream vacuum b-dots. I_{down} is the peak current measured by the downstream b-dots. I_{loss} is the peak of the difference between I_{up} and I_{down}.

Shot	Gap [mm]	V_{charge} [kV]	Vac Time [hr]	Vac_1 [torr]	Vac_2 [torr]	I_{up} [kA]	I_{down} [kA]	I_{loss} [kA]	I_{loss} [%]
9496	1.0	70.0	96	1.0E-06	1.3E-05	804.51	288.26	516.91	64.3%
9497	1.0	60.0	20	1.0E-06	1.1E-05	680.09	439.63	251.74	37.0%
9498	1.0	60.0	20	1.0E-06	1.2E-05	682.25	313.52	372.03	54.5%
9499	1.0	60.0	2.5	1.6E-06	1.6E-05	674.62	280.81	395.12	58.6%
9500	1.0	60.0	2.5	1.6E-06	1.7E-05	661.40	380.90	280.83	42.5%
9501	1.0	60.0	2.5	1.6E-06	1.6E-05	655.61	404.18	252.51	38.5%
9502	1.0	55.0	17	1.2E-06	1.1E-05	614.82	277.73	337.67	54.9%
9503	1.0	55.0	17	1.2E-06	1.1E-05	614.05	261.45	353.37	57.5%
9504	1.0	55.0	17	1.2E-06	1.1E-05	613.11	307.89	306.05	49.9%
9505	1.0	55.0	17	1.2E-06	1.1E-05	610.96	313.86	297.88	48.8%
9506	1.0	70.0	0.33	1.0E-04	1.1E-04	801.30	380.72	421.78	52.6%
9507	1.0	70.0	0.33	9.4E-05	1.0E-04	794.25	399.56	394.87	49.7%
9508	1.0	70.0	0.33	9.0E-05	1.0E-04	787.27	454.84	333.83	42.4%
9509	1.3	60.0	40	1.2E-06	9.6E-06	614.26	625.00	4.75	0.8%
9510	1.3	60.0	40	1.2E-06	9.6E-06	621.21	629.01	8.92	1.4%
9511	1.3	55.0	40	1.2E-06	9.6E-06	557.01	572.24	6.29	1.1%
9512	1.3	50.0	3	1.8E-06	2.0E-05	516.65	510.30	7.33	1.4%
9513	1.3	50.0	3	1.8E-06	2.0E-05	527.63	477.68	52.98	10.0%
9514	1.3	50.0	64	1.1E-06	1.0E-05	517.87	509.88	13.39	2.6%
9515	1.3	50.0	64	1.1E-06	1.0E-05	567.21	243.58	324.09	57.1%
9516	1.3	50.0	0.167	3.0E-05	1.0E-04	516.73	514.94	8.84	1.7%
9517	1.3	50.0	0.167	3.0E-05	1.0E-04	545.60	171.35	375.62	68.8%
9518	1.3	50.0	0	8.5E-02	8.5E-02	559.03	367.82	192.29	34.4%
9519	1.3	50.0	21	1.3E-06	1.0E-05	516.55	517.07	5.08	1.0%
9520	1.3	50.0	21	1.3E-06	1.0E-05	515.00	514.47	11.50	2.2%
9521	1.3	50.0	0.167	8.0E-06	9.3E-05	515.25	519.46	9.13	1.8%
9522	1.3	50.0	0.167	8.0E-06	9.0E-05	561.11	238.40	323.63	57.7%
9523	1.3	60.0	3	1.8E-06	1.8E-05	632.95	627.79	21.61	3.4%
9524	1.3	60.0	3	1.8E-06	1.8E-05	643.72	603.78	41.44	6.4%
9525	1.3	60.0	19	1.2E-06	1.3E-05	631.56	593.84	48.23	7.6%
9526	1.3	34.0	17	1.3E-06	1.1E-05	327.24	327.76	4.21	1.3%
9527	1.3	70.0	17	1.3E-06	1.1E-05	695.20	670.41	47.01	6.8%
9528	1.3	60.0	0.167	1.0E-05	1.0E-04	632.25	627.09	28.12	4.4%

Shot	Gap [mm]	Charge V [kV]	Vac Time [hr]	Vac 1 [torr]	Vac 2 [torr]	I up [kA]	I down [kA]	I loss [kA]	I loss [%]
9529	1.3	60.0	0.167	1.0E-05	8.5E-05	635.12	628.23	33.26	5.2%
9530	1.3	60.0	2	2.9E-06	2.6E-05	631.87	632.60	19.29	3.1%
9531	1.3	60.0	2	2.9E-06	2.6E-05	643.95	619.65	30.68	4.8%
9532	1.3	60.0	2	2.9E-06	2.6E-05	670.39	420.99	251.17	37.5%
9533	1.3	60.0	2	2.9E-06	2.6E-05	642.13	618.34	39.69	6.2%
9534	1.3	60.0	2	2.9E-06	2.6E-05	636.84	618.84	33.54	5.3%
9535	1.3	34.0	17	1.3E-06	1.1E-05	327.27	328.99	3.38	1.0%
9536	1.3	70.0	17	1.3E-06	1.2E-05	751.48	752.94	42.44	5.6%
9537	1.3	60.0	0.167	1.2E-05	8.5E-05	642.47	602.83	45.69	7.1%
9538	1.3	60.0	0.167	1.2E-05	8.5E-05	636.05	578.09	65.47	10.3%
9539	1.3	70.0	160	2.0E-06	8.5E-06	722.25	712.25	48.66	6.7%
9540	1.3	70.0	160	2.0E-06	8.5E-06	793.80	101.60	696.87	87.8%
9541	1.3	60.0	89	3.0E-06	1.0E-05	639.51	602.33	52.83	8.3%
9542	1.3	60.0	89	3.0E-06	1.2E-05	670.13	520.04	151.41	22.6%
9543	1.3	60.0	2	3.3E-06	1.8E-05	620.30	616.84	32.93	5.3%
9544	1.3	50.0	2	7.7E-06	2.8E-05	517.08	512.81	17.30	3.3%
9545	1.3	50.0	2	7.7E-06	2.8E-05	555.40	286.87	269.20	48.5%
9546	1.3	60.0	2.5	9.4E-06	2.2E-05	616.96	615.90	25.14	4.1%
9547	1.3	60.0	2.5	9.4E-06	2.2E-05	634.34	588.34	53.62	8.5%
9548	1.3	60.0	0.167	2.0E-05	9.8E-05	613.00	603.95	28.52	4.7%
9549	1.3	60.0	0.167	2.0E-05	9.8E-05	622.47	601.16	34.65	5.6%
9550	1.0	60.0	74	9.9E-07	1.3E-05	671.61	356.36	317.69	47.3%
9551	1.0	60.0	74	9.9E-07	1.3E-05	668.85	319.69	349.51	52.3%
9552	1.0	60.0	74	9.9E-07	1.3E-05	669.00	267.94	401.74	60.1%
9553	1.0	60.0	74	9.9E-07	1.3E-05	662.71	281.79	381.90	57.6%
9554	1.0	60.0	74	9.9E-07	1.3E-05	673.24	260.18	413.82	61.5%
9555	1.0	60.0	0.167	2.0E-05	1.0E-04	664.88	404.63	262.42	39.5%
9556	1.0	60.0	0.167	2.0E-05	1.0E-04	666.53	300.63	366.22	54.9%
9557	1.0	60.0	0.167	2.0E-05	1.0E-04	665.45	396.32	271.26	40.8%
9558	1.0	60.0	0.167	2.0E-05	1.0E-04	671.61	361.59	312.01	46.5%
9559	1.0	60.0	0.167	2.0E-05	1.0E-04	663.95	318.49	345.90	52.1%
9560	1.0	60.0	0.167	2.0E-05	1.0E-04	663.05	315.42	349.20	52.7%

References

[1] W. A. Stygar, P. A. Corcoran, H. C. Ives, R. B. Spielman, J. W. Douglas, B. A. Whitney, M. A. Mostrom, T. C. Wagoner, C. S. Speas, T. L. Gilliland, G. A. Allshouse, R. E. Clark, G. L. Donovan, T. P. Hughes, D. R. Humphreys, D. M. Jaramillo, M. F. Johnson, J. W. Kellogg, R. J. Leeper, F. W. Long, T. H. Martin, T. D. Mulville, M. D. Pelock, B. P. Peyton, J. W. Poukey, J. J. Ramirez, P. G. Reynolds, J. F. Seamen, D. B. Seidel, A. P. Seth, A. W. Sharpe, R. W. Shoup, J. W. Smith, D. M. Van De Valde, and R. W. Wavrik, "55-TW magnetically insulated transmission-line system: Design, simulations, and performance," *Physical Review Special Topics - Accelerators and Beams*, vol. 12, no. 12, p. 120401, 2009, PRSTAB.

[2] T. D. Pointon and M. E. Savage, "2-D PIC Simulations of Electron Flow in the Magnetically Insulated Transmission Lines of Z and ZR," in *Pulsed Power Conference, 2005 IEEE*, 2005, Conference Proceedings, pp. 151–154.

[3] D. V. Rose, D. R. Welch, T. P. Hughes, R. E. Clark, and W. A. Stygar, "Plasma evolution and dynamics in high-power vacuum-transmission-line post-hole convolutes," *Physical Review Special Topics - Accelerators and Beams*, vol. 11, no. 6, p. 060401, 2008, PRSTAB.

[4] J. P. Martin, M. E. Savage, T. D. Pointon, and M. A. Gilmore, "Tailoring of electron flow current in magnetically insulated transmission lines," *Physical Review Special Topics - Accelerators and Beams*, vol. 12, no. 3, p. 030401, 2009, PRSTAB.

[5] J. M. Creedon, "Relativistic brillouin flow in the high mu/gamma diode," *Journal of Applied Physics*, vol. 46, no. 7, pp. 2946–2955, 1975.

[6] J. M. Creedon, "Magnetic cutoff in high current diodes," *Journal of Applied Physics*, vol. 48, no. 3, pp. 1070–1077, 1977.

[7] C. W. Mendel, D. B. Seidel, and S. E. Rosenthal, "A simple theory of magnetic insulation from basic physical considerations," *Laser and Particle Beams*, vol. 1, no. 03, pp. 311–320, 1983.

[8] W. A. Stygar, T. C. Wagoner, H. C. Ives, P. A. Corcoran, M. E. Cuneo, J. W. Douglas, T. L. Gilliland, M. G. Mazarakis, J. J. Ramirez, J. F. Seamen, D. B. Seidel, and R. B. Spielman, "Analytic model of a magnetically insulated transmission line with collisional flow electrons," *Physical Review Special Topics - Accelerators and Beams*, vol. 9, no. 9, p. 090401, 2006, PRSTAB.

[9] J. P. VanDevender, R. W. Stinnett, and R. J. Anderson, "Negative ion losses in magnetically insulated vacuum gaps," *Applied Physics Letters*, vol. 38, no. 4, pp. 229–231, 1981.

[10] R. W. Stinnett and T. Stanley, "Negative ion formation in magnetically insulated transmission lines," *Journal of Applied Physics*, vol. 53, no. 5, pp. 3819–3823, 1982.

[11] R. W. Stinnett, M. A. Palmer, R. B. Spielman, and R. Bengtson, "Small gap experiments in magnetically insulated transmission lines," *Plasma Science, IEEE Transactions on*, vol. 11, no. 3, pp. 216–219, 1983.

[12] R. Presura, B. S. Bauer, A. Esaulov, S. Fuelling, V. Ivanov, N. Le Galloudec, V. Makhin, R. E. Siemon, V. I. Sotnikov, R. Wirtz, A. Astanovitsky, S. Batie, H. Faretto, B. Le Galloudec, A. Oxner, M. Angelova, P. Laca, S. Guzzetta, S. Keely, S. Rogowski, B. V. Oliver, and K. W. Struve, "Operation regimes of magnetically insulated transmission lines," in *Pulsed Power Conference, 2003. Digest of Technical Papers. PPC-2003. 14th IEEE International*, vol. 2, 2003, Conference Proceedings, pp. 859–862 Vol.2.

[13] V. V. Ivanov, P. J. Laca, B. S. Bauer, R. Presura, V. I. Sotnikov, A. L. Astanovitskiy, B. Le Galloudec, J. Glassman, and R. A. Wirtz, "Investigation of plasma evolution in a coaxial small-gap magnetically insulated transmission line," *Plasma Science, IEEE Transactions on*, vol. 32, no. 5, pp. 1843–1848, 2004.

[14] Y. L. Bakshaev, A. V. Bartov, P. I. Blinov, A. S. Chernenko, S. A. Danko, Y. G. Kalinin, A. S. Kingsep, V. D. Korolev, V. I. Mizhiritskii, V. P. Smirnov, A. Y. Shashkov, P. V. Sasorov, and S. I. Tkachenko, "Study of the dynamics of the electrode plasma in a high-current magnetically insulated transmission line," *Plasma Physics Reports*, vol. 33, no. 4, pp. 259–270, 2007.

[15] J. Halbritter, "On contamination on electrode surfaces and electric field limitations," *Electrical Insulation, IEEE Transactions on*, vol. EI-20, no. 4, pp. 671–681, 1985.

[16] M. E. Cuneo, "The effect of electrode contamination, cleaning and conditioning on high-energy pulsed-power device performance," *Dielectrics and Electrical Insulation, IEEE Transactions on*, vol. 6, no. 4, pp. 469–485, 1999.

[17] W. A. Stygar, M. E. Savage, and M. C. Jones, "Analytic model of the Z vacuum system," 2013 Dec 6, Internal Memo, unpublished.

[18] A. Kim, S. Frolov, V. Alexeenko, V. Sinebryukhov, M. Mazarakis, and F. Bayol, "Prefire probability of the switch type Fast LTD," in *Pulsed Power Conference, 2009. PPC '09. IEEE*, 2009, Conference Proceedings, pp. 565–570.

[19] A. A. Kim, M. G. Mazarakis, V. A. Sinebryukhov, B. M. Kovalchuk, V. A. Visir, S. N. Volkov, F. Bayol, A. N. Bastrikov, V. G. Durakov, S. V. Frolov, V. M. Alexeenko, D. H. McDaniel, W. E. Fowler, K. LeChien, C. Olson, W. A. Stygar, K. W. Struve, J. Porter, and R. M. Gilgenbach, "Development and tests of fast 1-MA linear transformer driver stages," *Physical Review Special Topics - Accelerators and Beams*, vol. 12, no. 5, p. 050402, 2009, PRSTAB.

[20] K. LeChien, M. Mazarakis, W. Fowler, W. Stygar, F. Long, R. McKee, G. Natoni, J. Porter, K. Androlewicz, T. Chavez, G. Feltz, V. Garcia, D. Guthrie, R. Mock, T. Montoya, J. Puissant, A. Smith, P. Wakeland, K. Ward, D. Van De Valde, and A. Kim, "A 1-MV, 1-MA, 0.1-Hz linear transformer driver utilizing an internal water transmission line," in *Pulsed Power Conference, 2009. PPC '09. IEEE*, 2009, Conference Proceedings, pp. 1186–1191.

[21] M. G. Mazarakis, M. E. Savage, W. E. Fowler, L. F. Bennett, M. Jones, F. W. Long, M. K. Matzen, D. H. McDaniel, R. G. McKee, J. L. McKenney, J. L. Porter, B. S. Stoltzfus, K. W.

Struve, W. A. Stygar, J. R. Woodworth, A. A. Kim, V. A. Sinebryukhov, K. L. LeChien, P. Wakeland, K. Ward, J. G. Puissant, T. F. Chavez, P. A. Jones, D. J. Lucero, G. Natoni, and S. A. Lewis, "Experimental validation of the first 1-MA water-insulated MYKONOS LTD voltage adder," in *Pulsed Power Conference (PPC), 2011 IEEE*, 2011, Conference Proceedings, pp. 625–628.

[22] M. E. Savage, M. G. Mazarakis, K. R. LeChien, B. S. Stoltzfus, W. A. Stygar, W. E. Fowler, E. A. Madrid, C. L. Miller, and D. V. Rose, "Temporally shaped current pulses on a two-cavity linear transformer driver system," in *Pulsed Power Conference (PPC), 2011 IEEE*, 2011, Conference Proceedings, pp. 844–849.

[23] T. C. Wagoner, W. A. Stygar, H. C. Ives, T. L. Gilliland, R. B. Spielman, M. F. Johnson, P. G. Reynolds, J. K. Moore, R. L. Mourning, D. L. Fehl, K. E. Androlewicz, J. E. Bailey, R. S. Broyles, T. A. Dinwoodie, G. L. Donovan, M. E. Dudley, K. D. Hahn, A. A. Kim, J. R. Lee, R. J. Leeper, G. T. Leifeste, J. A. Melville, J. A. Mills, L. P. Mix, W. B. S. Moore, B. P. Peyton, J. L. Porter, G. A. Rochau, G. E. Rochau, M. E. Savage, J. F. Seamen, J. D. Serrano, A. W. Sharpe, R. W. Shoup, J. S. Slopek, C. S. Speas, K. W. Struve, D. M. Van De Valde, and R. M. Woodring, "Differential-output B-dot and D-dot monitors for current and voltage measurements on a 20-MA, 3-MV pulsed-power accelerator," *Physical Review Special Topics - Accelerators and Beams*, vol. 11, no. 10, p. 100401, 2008, PRSTAB.

[24] W. A. Stygar, W. E. Fowler, K. R. LeChien, F. W. Long, M. G. Mazarakis, G. R. McKee, J. L. McKenney, J. L. Porter, M. E. Savage, B. S. Stoltzfus, D. M. Van De Valde, and J. R. Woodworth, "Shaping the output pulse of a linear-transformer-driver module," *Physical Review Special Topics - Accelerators and Beams*, vol. 12, no. 3, p. 030402, 2009, PRSTAB.